

Chapter 5

THE TRANSITION-EDGE MICROBOLOMETER (TREMBOL)

Operation of detectors at low temperatures has the advantages of lower noise and better thermal conditions. But detector responsivity for conventional bolometers suffers from a drop in α as the temperature is lowered. The large α for a superconductor at its transition between normal conductivity and superconductivity makes it an ideal detector material for low temperature applications. Figure 5.1 shows the resistive transition of a 250 mil long by 50 mil wide lead resistor. This transition is very steep, with a dR/dT of about $3.7 \text{ } \Omega/\text{K}$. If a Pb detector could be biased near the center of this transition, it could be highly responsive. However, it may be difficult to control temperature to the center of such a narrow transition.

In this chapter, the transition-edge microbolometer (TREMBOL) is introduced. Following a brief background over superconducting bolometers, a TREMBOL structure will be presented which uses the low transition temperature (T_c) element Pb as the superconductor. Then, several structures will be presented which could result in useful devices. The equipment used to test these devices near liquid helium temperatures is then described. The chapter concludes with directions for future research.

5.1 Background of Superconducting Bolometers

Both conventional and composite superconducting bolometers have been fabricated. Conventional-type superconducting bolometers are large area structures where the detector film also acts as the radiation absorber. These have been built using tin [¹⁻²³⁴] and niobium nitride [⁵⁻⁶⁷]. The first bolometer to actually utilize the superconducting transition was a composite structure using a blackened aluminum foil absorber in conjunction with a tantalum temperature sensor [⁸]. Another such composite structure makes use of aluminum as the temperature sensor and bismuth

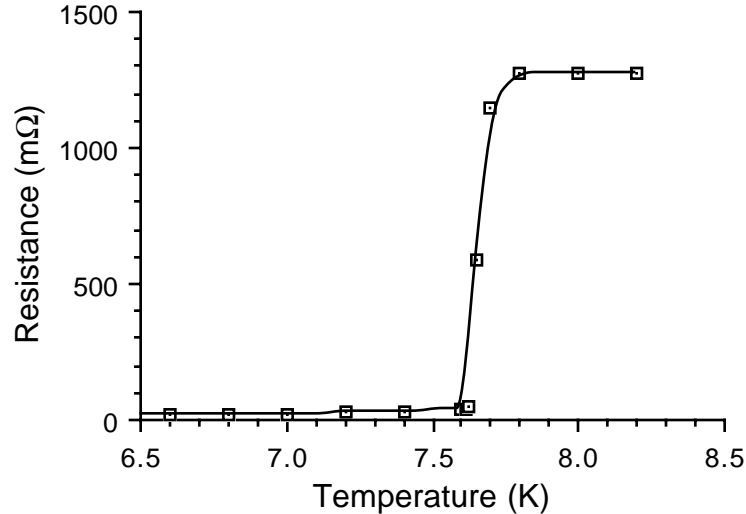


Fig. 5.1: The resistive transition for a 50 mil wide, 250 mil long, 1000 Å thick Pb resistor.

as the absorber [9]. Recently, an infrared detector which utilizes a weak-link mechanism rather than a bolometric type mechanism has been fabricated using a bulk high transition temperature superconductor (HT_cS) [10]. Other works have focussed on using superconductors for optical and far-infrared detectors [11-12131415].

The feasibility of a conventional-type bolometer using the transition of a HT_cS film has been discussed by Richards, *et al.* [16]. They obtained estimates of the sensitivity for such a bolometer by carefully measuring the resistance and the low frequency noise in the transition region of several HT_cS samples. By assuming that sensitivity is not limited by thermal conductance out of the device, a noise equivalent power (NEP) as low as $10^{-12} \text{ W}/\sqrt{\text{Hz}}$ was postulated.

The idea of coupling a small superconducting bolometer to a planar integrated antenna was first suggested by Neikirk [17]. An antenna-coupled superconducting bolometer structure must perform three functions. It must absorb power from the antenna (i.e. it must provide a matched **load** to the antenna impedance). It must sense temperature changes due to the absorbed power (i.e. there must be a thermal **detector**). And finally, it must bias the superconductor to its transition

temperature. If the ambient temperature is maintained below the transition temperature, a **heater** can be used to provide this bias. These three elements are not necessarily separate. In the simplest configuration of the TREMBOL, for instance, the superconducting film would act as both the load and the detector. In this case, the heater must be separate, and most likely would control the overall temperature to bias the entire array at the transition point. Such a TREMBOL is discussed in section 5.2 using lead as the superconducting material. The feasibility of a HT_cS TREMBOL structure with an NEP as low as $2.5 \times 10^{-12} \text{ W}/\sqrt{\text{Hz}}$ has recently been discussed by Hu and Richards [18].

A problem with this simplest configuration of the TREMBOL is that the superconducting thin film resistivity throughout the transition region may be too low to provide a matched load to the antenna. A $4 \mu\text{m} \times 4 \mu\text{m}$ square of 1000 Å thick YBCuO type superconducting thin film would have a transition region resistance of no higher than about 20 Ω. Typical planar antennas, on the other hand, generally have impedances in the 100 - 300 Ω range. One structure which could possibly match to a HT_cS resistor is a twin slot antenna [19, 20] which is separated from the detector by a thin dielectric. It is theoretically possible to achieve antenna impedances as low as 5 Ω with these slot antennas.

Two other ways to overcome the matched load problem are to place the superconducting detector in series contact with a resistive load, or to build a composite TREMBOL structure. These methods are discussed in sections 5.3 and 5.4.

5.2 The TREMBOL using a Conventional Superconductor

To investigate the TREMBOL, a lead detector element coupled to a bow-tie antenna was fabricated. Pb was chosen as the detector material because its transition temperature is above the boiling point of liquid He, and because it is easy to evaporate. TREMBOLs made with niobium and lead bismuthide were also attempted. However, fabrication of a good Nb superconductor requires high vacuum and rapid evaporation rates, conditions very difficult to obtain in our vacuum system. Also, even though PbBi is easy to evaporate, it forms a discontinuous film unless it is evaporated on a cold substrate (on the order of 77 K).

Pb is not without its own problems; our devices oxidized and became useless after about 48 hours of exposure to air.

The devices fabricated were $4.5\ \mu\text{m}$ long, $5.0\ \mu\text{m}$ wide, and $1000\ \text{\AA}$ thick Pb. Prior to device fabrication, gold contact pads were electroplated on the glass substrate. The antenna metal was gold, and chrome was used to promote adhesion. The Pb detector/Au antenna devices were fabricated using the photoresist bridge technique described in chapter 3. Following liftoff, the chip was stored in a desiccator to slow down oxidation of the Pb elements. Immediately prior to testing, the devices were wire-bonded to the printed circuit board used in the cryogenic testing apparatus. Aluminum wire was used, since it bonds quite easily to electroplated gold. Figure 5.2 shows the placement of the wire bonds to the tested TREMBOL. For maximum accuracy, a 4 point current-voltage test is desired as close as possible to the superconducting element.

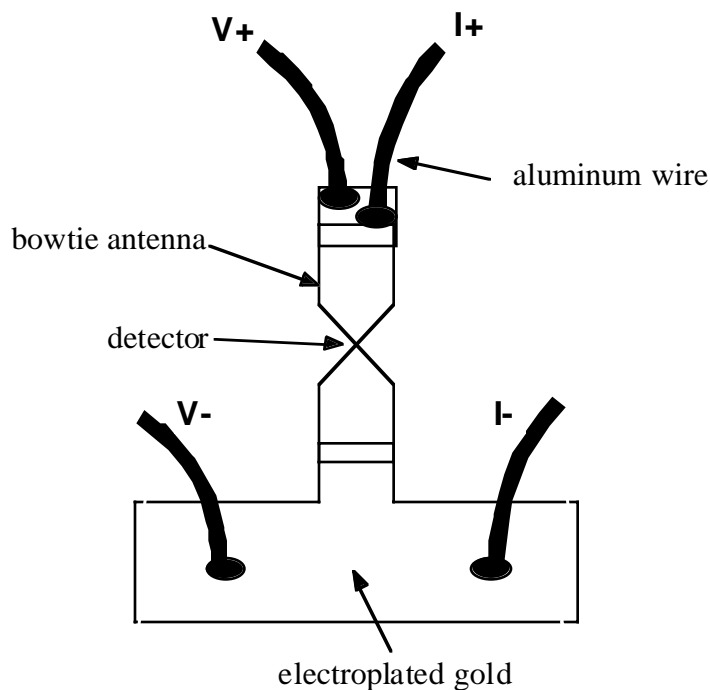


Fig. 5.2: The 4-point measurement setup for the Pb TREMBOL. Aluminum wire is thermosonically bonded to electroplated gold contact pads.

Preliminary evaluation of the TREMBOL requires a resistance plot across the transition, and the resistance across the device as a function of power dissipated in the element (Chapter 2 discussed how these parameters can give the dc responsivity of a microbolometer). Figure 5.3 shows the Pb TREMBOL's resistive transition. The resistance was calculated based on the slope of the I-V curve from 0 to 1 mA at each temperature tested. Notice that there is a 'foot' at the base of the transition which was not present for the larger Pb resistor R-T plot of Fig. 5.1. This is most likely 'weak-link' type behavior, resulting from finite sized crystals in the small detector. The dR/dT slope in the region represented by the dashed line is $3.6 \text{ } \Omega/\text{K}$, which is about the same as for the larger resistor of Fig. 5.1.

The resistance of the TREMBOL as a function of power dissipated is shown in Fig. 5.4 at three temperatures near the transition. If the device is biased at too low a temperature (the curve for 7.46 K), the detector will remain superconducting, and there will be no Joule-heating of the element. Thus, no transition is seen for the 7.46 K plot. At 7.66 K, the device is biased at a high enough temperature to experience the transition. At 7.75 K, which lies just about in the center of the

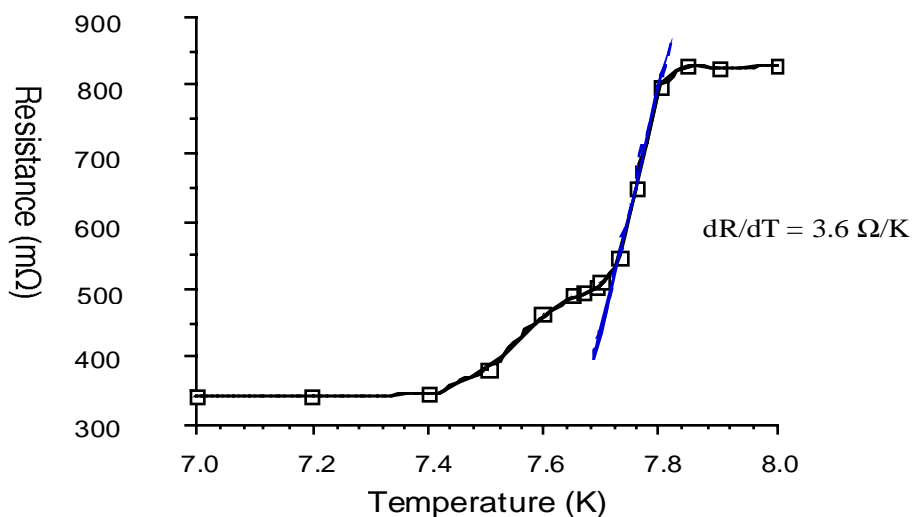


Fig. 5.3: The resistive transition for the $4.5 \text{ } \mu\text{m}$ long, $5.0 \text{ } \mu\text{m}$ wide, $1000 \text{ } \text{Å}$ thick Pb TREMBOL.

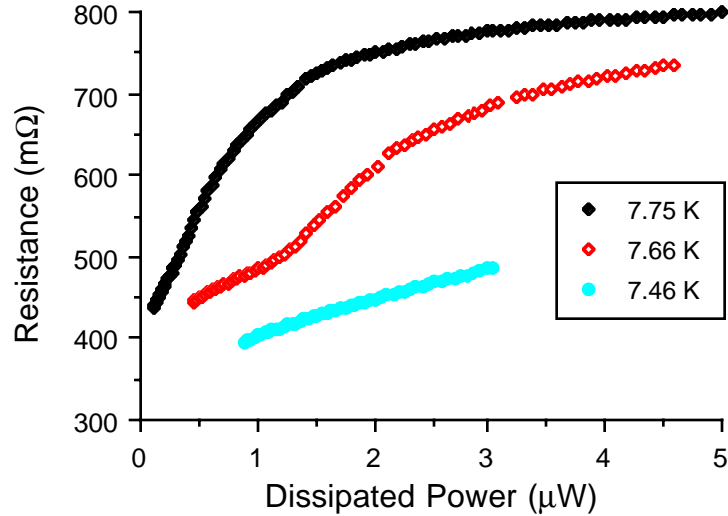


Fig. 5.4: Resistance-Power plots at various temperatures near the transition for the Pb TREMBOL.

dashed transition region shown in Fig. 5.3, the dR/dP plot starts out quite steep. It levels off because at sufficient power dissipated, the device is driven beyond the transition region. The parameters of interest for this device are summarized in Table 5.1. Best dc responsivity of 274 V/W was calculated at 7.75 K.

The TREMBOL has also been examined using the simple thermal model developed in chapter 2. One significant difference is that the dR/dT slope for a superconductor is positive and very steep compared to the dR/dT slopes of Bi and Te. The model responded to the steep slope by undergoing a thermal runaway when just the dR/dT slope was considered. That is, as temperature rose within a finite element of the detector, its resistance increased. This increased resistance produced more heat for a given bias current, resulting in higher temperature, etc. To prevent this thermal runaway, the leveling off of resistance at the top of the transition was included in the model. Since the thermal conductivity of the antenna metal is very high at cryogenic temperatures, the peak temperature in the Pb element reached only to about the top of the transition (about 7.81 K) for the 7.75 K ambient case of Table 5.1. The glass substrate thermal conductivity is very low at this

	Temperature (K)	Bias current (mA)	dR/dP (kΩ/W)	Z _{th} (K/mW)	r _{dc} (V/W)
Pb:	7.66	1.75	138	38	242
	7.75	1.0	274	76	274
Bi:	300	1.0	-20	-67	-20

Table 5.1: Performance of the Pb TREMBOL operated near the middle of the transition regions shown in Fig. 5.4. dR/dP is the slope in the steepest region of each plot, centered at the bias current given. Also calculated is the thermal impedance Z_{th}, and the responsivity r_{dc}. For comparison, values for a room temperature Bi microbolometer are included [17].

temperature, so there was little heat conduction into the substrate. For higher temperature rises, and therefore higher responsivities, a superconductor with lower thermal conductivity is desired.

In actual operation, the Pb TREMBOL would have a severe problem coupling to the bow-tie antenna since its middle of the transition resistance is only about 700 mΩ. The following two sections suggest methods for improving coupling of these kind of low resistance detectors to planar antennas.

5.3 The TREMBOL with Series-Added Resistance

One way to overcome the mismatched load problem is to place the superconducting detector in series contact with a resistive load, as shown in Fig. 5.5. The series resistance combination would form a load matched to the antenna. As a rule of thumb, such a structure would only be feasible if the resistance of the superconducting portion (in the middle of its transition) is no less than one-tenth the value of the resistive load. Some of the high temperature superconductors have resistances high enough for this purpose.

If a TREMBOL structure is considered which has a HT_cS film in series with a load resistance, the temperature coefficient of resistance α_{TR} for the complete device can be estimated. The literature reports a considerable range of resistivity values for HT_cS films. A rather high value of ρ = 200 μΩ-cm has been reported [16] which leads to a resistance of 20 Ω for a 1000 Å thick square of HT_cS material. If this is

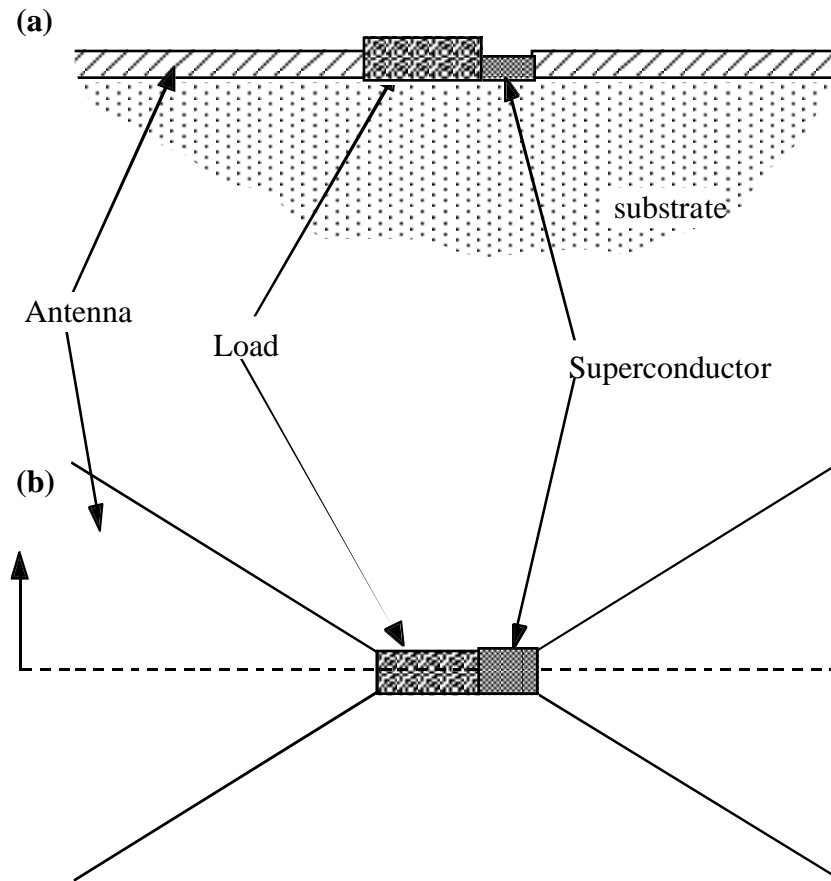


Fig. 5.5: TREMBOL structure where the superconducting detector is series connected with a resistor to create a load impedance matched to the antenna.

placed in series with an 80Ω resistor (assumed to have a zero α), and assuming an α for the HTcS film of 0.5 K^{-1} , then α_{TR} is calculated to be 0.10 K^{-1} .

The responsivity of a TREMBOL which has a HTcS detector placed in series with a load resistor can be compared to the responsivity of a bismuth microbolometer. Responsivity r in volts per watt is given by

$$r = V_b \alpha Z_T \quad (5.1)$$

where V_b is the voltage bias across the bolometer, α is the temperature coefficient of resistivity in K^{-1} , and Z_T is the thermal impedance of the device in degrees K per watt. Z_T is approximately the inverse of the thermal conductance out of the device, and depends on the thermal conductances of the substrate, detector, and antenna materials. It is also dependent on the device thermal mass, but this effect can be ignored for low modulation frequencies. Assuming that V_b and Z_T are about the same for both the bismuth microbolometer and the TREMBOL, then the TREMBOL's responsivity r_{TR} is related to the bismuth microbolometer's responsivity r_{Bi} by

$$\frac{r_{TR}}{r_{Bi}} = \frac{\alpha_{TR}}{\alpha_{Bi}} \quad (5.2)$$

where α_{TR} and α_{Bi} are for the TREMBOL and the bismuth microbolometer, respectively. A typical thin bismuth film has an $\alpha = -0.003 K^{-1}$. The TREMBOL structure with series added resistance therefore has the potential for thirty times better responsivity than a conventional Bi microbolometer.

Two other considerations need to be mentioned concerning this comparison. First, it is not clear how much bias current a HT_cS TREMBOL can handle in the transition region. A bismuth film can handle up to $10^6 A/cm^2$. Therefore, unless the HT_cS film can withstand such current densities (which are near the maximum values reported in the literature), the performance ratio will be less. Second, a driving force behind the TREMBOL is the need for a sensitive broad-band detector of far-infrared radiation. Sensitivity of such a device is improved at low operating temperatures because there is less thermal noise. The TREMBOL would operate in the temperature vicinity of liquid nitrogen; the comparison above considers the responsivity of a Bi microbolometer at room temperature. Actually, at liquid nitrogen temperature the magnitude of α_{Bi} is much lower [²¹], and r_{Bi} will therefore be much smaller.

5.4 Composite TREMBOL

Another solution to the mismatched load problem is to separate the load from the detector in a composite TREMBOL structure (Fig. 5.6). This type of device follows from the research using Te as the detecting element in a room-temperature antenna-coupled composite microbolometer [22]. The load, which is matched to the antenna, may now also serve as the heater by applying a dc bias through the antenna leads. The superconducting detector element is in intimate thermal contact with, but is electrically isolated from, the load/heater element. Changes in heater temperature will be quickly followed by changes in detector temperature. As the detector changes temperature in the transition region, large changes in resistance will occur, which are measured with a current biasing circuit. Using the kind of analysis found in section 5.3, the TREMBOL should have a responsivity almost two orders of magnitude greater than that of a bismuth microbolometer.

An advantage of this device is that the entire substrate can be cooled to below the transition temperature, and the detector can be "turned on" by applying a biasing current through the heater element. This can be quite useful for multiplexing as discussed in section 5.4.1. The superconducting film may also be used as a low-loss signal line away from the detector, since the entire structure is cooled to below the transition temperature. The device speed is limited by both the thermal mass of the heating element and by the thermal conductance between the heater and the detector. The detectable FIR frequency will be limited by the detector to load capacitance, and therefore the overlap area must be kept small. For a $4\ \mu\text{m} \times 4\ \mu\text{m}$ detector separated from the load by $1000\ \text{\AA}$ of SiO_2 , capacitance limits operation to below 100 GHz (see section 5.4.2).

Fabrication of the composite TREMBOL involves a choice of superconducting and resistive heater materials. The resistance of the heater material must be known over the temperature range of interest, and the proper dimensions must be chosen to achieve an impedance match with the antenna. Resistive heater candidates include nichrome and bismuth. Superconducting materials include the low T_c superconductors (such as tin, niobium, lead, and lead bismuthide), and the new high transition temperature superconductors. The HT_cS materials, primarily

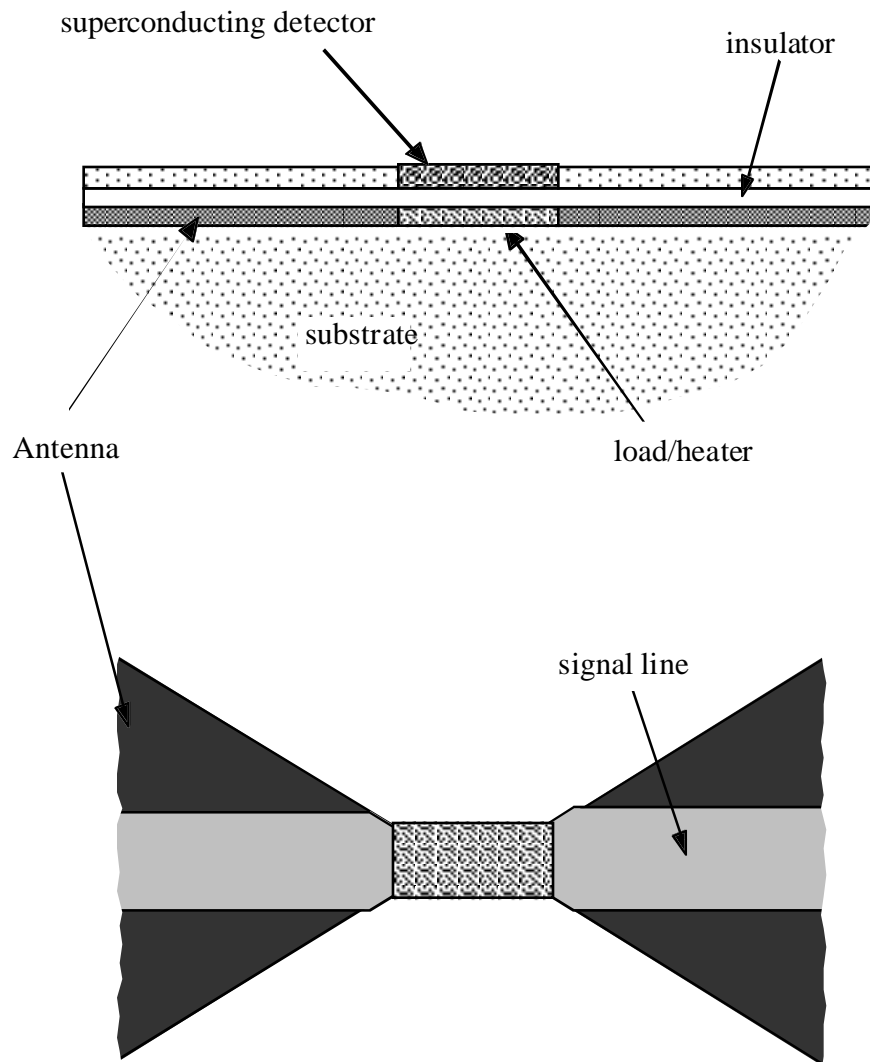


Fig. 5.6: Cross section (a) and top view (b) of a composite TREMBOL. Radiation is coupled into the load/heater by the planar antenna structure, causing a rise in the temperature of the load. Due to the intimate thermal contact between the load and the superconducting detector, the resistance of the TREMBOL changes. This resistance change is sensed by the signal line.

YBaCuO compositions and related compounds, were discovered by Bednorz and Müller [23], and improved upon by a host of researchers (see [24, 25] and references contained therein). A variety of techniques can be used to deposit thin films of these materials [26-2728]. One way to fabricate a composite TREMBOL would be to use a photoresist lift-off technique for patterning the superconducting thin film. Following the deposition, patterning, and high temperature anneal of this film, a thin (1000-2000 Å) layer of silicon nitride or silicon dioxide would be deposited over the superconductor. This layer would serve as the electrical insulator, but is thin enough to be a good thermal conductor. Finally, the antenna/heater would be fabricated by the usual photoresist bridge technique used to make bismuth microbolometers [29].

Consideration must also be given to annealing and substrate effects, since some of the more commonly cited substrate materials upon which superconducting thin films are deposited (such as strontium titanate) are not particularly good rf substrates. The more common substrates used in microwave circuits have thus far produced inferior YBaCuO films; for instance, sapphire tends to dope the YBaCuO with Al during the high temperature anneal, which seriously degrades the film. Recently, however, a high T_c superconductor was successfully deposited on a LaAlO₃ substrate [30], which has desirable rf properties.

5.4.1 Matrix Addressing in a Composite TREMBOL Array

There are a variety of applications for microbolometer arrays in the FIR spectral region that require imaging, which is the mapping of the radiation intensity of a distributed source [31, 32]. A single detector with mechanically scanned optics may be too slow to build up an image, especially in applications where the required integration time is long (astronomy), or where events occur quickly (plasma diagnostics). Thus, an array of detectors is highly desirable for imaging. A number of one dimensional line arrays have been fabricated using conventional bismuth microbolometers [33]. To image two dimensional objects, however, these line arrays still require mechanical scanning in the direction orthogonal to the array axis.

Two dimensional arrays using conventional microbolometers have proven to be very difficult to design, since it is not possible to matrix address resistors. A

unique feature of the composite TREMBOL, however, would allow each individual detector in a 2-D array to be matrix addressed. Figure 5.7 shows a simple 3 x 4 array where each TREMBOL heater is connected to two address lines (row and column), and the detector element is connected to a signal line. If the entire array is chilled to below the superconducting transition temperature, then without an applied heater bias the detectors will act as electrical shorts. A specific detector may be turned on by setting the appropriate pair of heater address lines high and low. Only the signal generated by the activated detector will be transmitted out the signal line since all the other detectors on the line will be at zero resistance. In actual operation, a clocked cycle could be used to sample data out of one row at a time.

Proper operation of a TREMBOL array would require that each device be biased at its transition temperature. This may be difficult in an array where the heater resistance will vary from device to device. In this case, a look-up table could be used to set each device's bias across the heater to a predetermined optimum value.

5.4.2 Capacitive Roll-Off in a Composite TREMBOL

A capacitance exists between the superconducting detector and the load/heater of the composite TREMBOL which will set an upper limit on the frequency of radiation it can detect. An electrical representation of the composite structure is shown in Fig. 5.8. In this figure, R_h is the load/heater resistor, R_d is the resistance of the HT_CS detector, and C is the capacitance between the load/heater and the HT_CS detector. Assuming the simplest case where the impedance of the antenna is purely real (i.e. the antenna is resonant),

$$Z_{\text{ant}} = \frac{1}{\frac{1}{R_h} + \frac{1}{\left| R_d + \frac{1}{j\omega C} \right|}} = \frac{1}{\frac{1}{R_h} + \frac{1}{|Z_d|}} \quad (5.3)$$

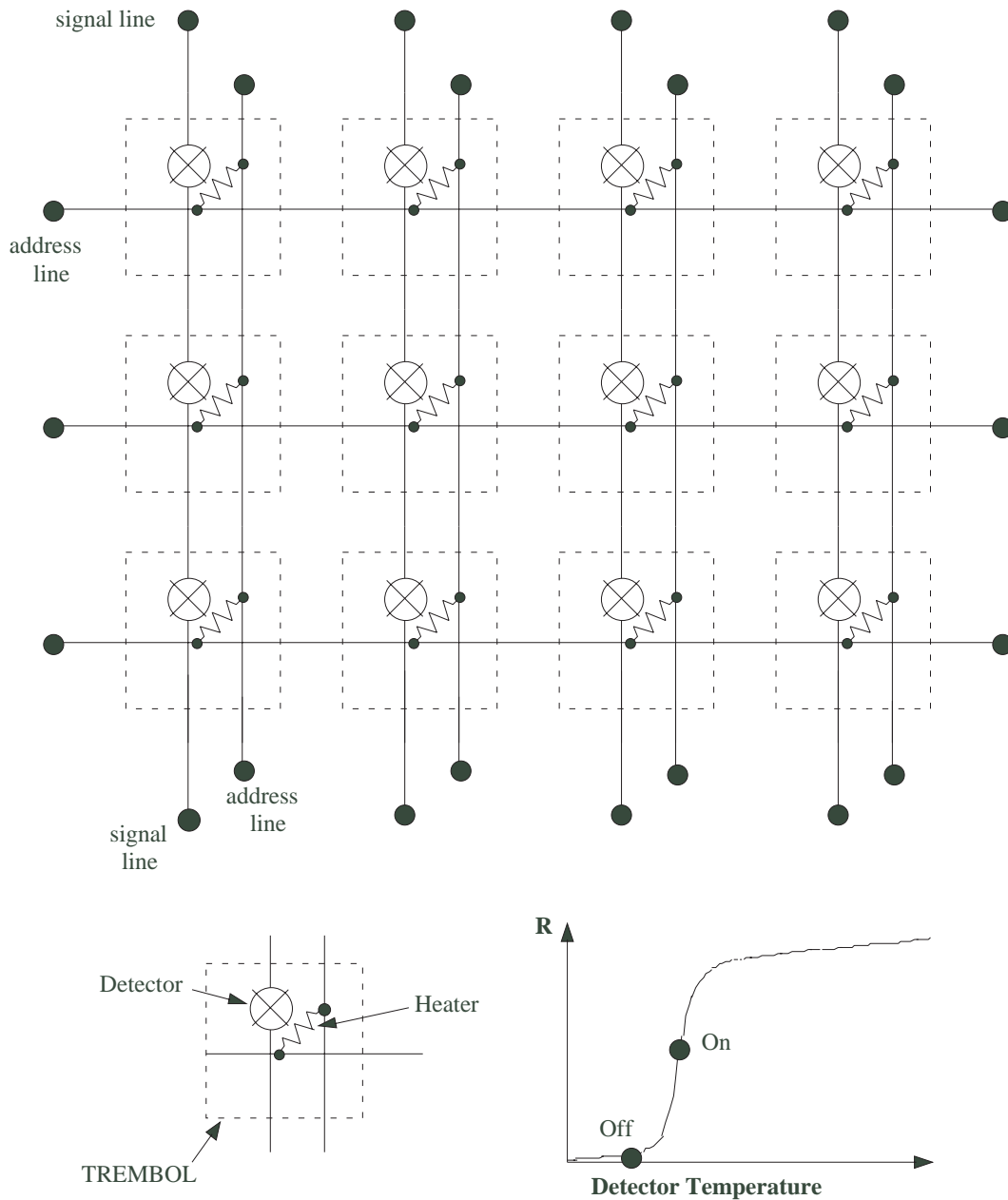


Fig. 5.7: Multiplexing in a composite TREMBOL array. A 3 x 4 array is shown where each device consists of a heater connected to two address lines and a detector connected to a signal line. The device is turned on by applying enough heat to bring the detector to the center of the transition region.

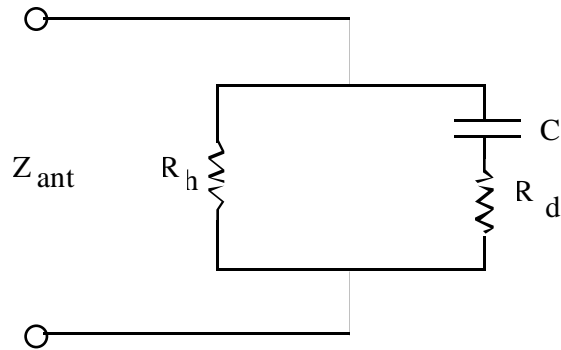


Fig. 5.8: Equivalent circuit of a composite TREMBOL. For maximum transmission of energy, the antenna impedance Z_{ant} is matched to the parallel combination of the load/heater resistance R_h and the detector impedance $R_d + (j\omega C)^{-1}$.

where Z_{ant} is the antenna impedance, ω is the angular frequency, and the magnitude of the detector impedance Z_d is indicated by absolute value bars. The capacitance C is desired minimum, and is given by

$$C = \frac{\epsilon_r \epsilon_0 A}{d} \quad (5.4)$$

where an insulator of thickness d and relative dielectric constant ϵ_r separates the load/heater from the HT_cS detector, which has an area A . If a 1000 Å thick layer of SiO₂ is used as the electrical insulator, and the area is 4 μm x 4 μm, then $C = 5.4 \times 10^{-15}$ F. The area considered in this example is a minimum capacitive area, assuming a signal line running perpendicular to the direction of the bow. In the present TREMBOL configuration, the signal line runs along the top of the antenna, which would result in a severe capacitance problem.

The HT_cS detector resistance for a 1000 Å thick square with $\rho = 200 \mu\Omega\text{-cm}$ is just 20 Ω. Using these values, the magnitude of the detector impedance is determined for several frequencies below. If the heater/load resistance is chosen as 100 Ω, then the total impedance of the composite TREMBOL, $R_h \parallel Z_d$, can be calculated. This data shows that reasonable coupling is possible between an antenna of impedance 100 Ω and the composite TREMBOL for frequencies below

100 GHz. However, given the present composite TREMBOL configuration with the signal line lying atop the bow arms, the capacitance could prove fatal. More study is needed to verify the feasibility of this device.

frequency (Hz)	$ Z_d $ (Ω)	$R_h Z_d$ (Ω)
10^{10}	3000	97
10^{11}	300	75
10^{12}	36	26
10^{13}	20	17

Table 5.2: Composite TREMBOL impedance as a function of frequency.

5.5 Cryogenic Apparatus

Operation of superconducting detectors requires a low temperature environment. This low temperature has been achieved for the most part by using liquid He (boiling point 4.2 K) for low T_c superconductors, and liquid nitrogen (boiling point 77.3 K) for the high T_c superconductors. Closed cycle refrigerator systems are also used. These are especially important in space applications, where replacement of liquid coolant is impractical. These units are typically multistage refrigerators employing a Joule-Thompson expansion [³⁴⁻³⁵³⁶].

In the study of the low T_c superconducting TREMBOL, liquid He was used to achieve temperatures down to 5 K. A sample rod was built which allows control of substrate temperature while immersed in liquid Helium. A simple sketch of the dewar assembly and sample rod is shown in Fig. 5.9. Prior to immersion, the sample rod is evacuated and flushed several times with He gas. Then, it is precooled by immersing in liquid nitrogen. After slowly inserting the cooled rod into the He dewar, the pressure of He gas is increased to about 1 torr. This gas provides for most of the thermal conduction between the outer walls of the sample assembly and the copper sample plate. The low thermal conductivity of stainless steel provides a good thermal barrier to the outside ambient temperature.

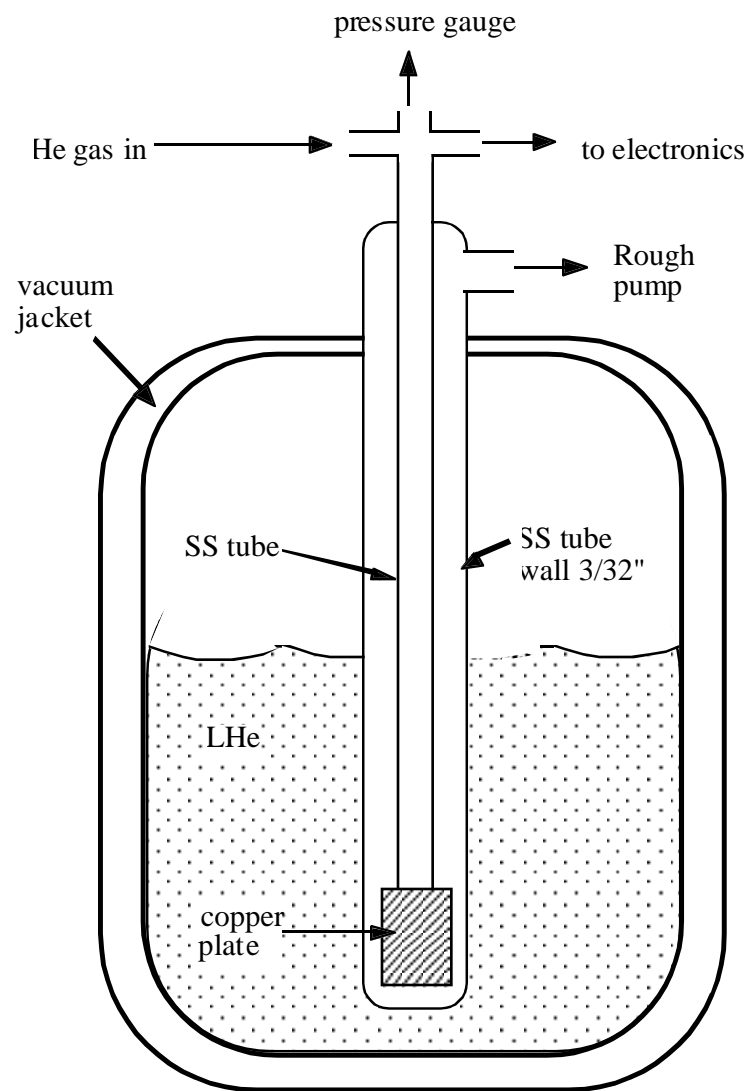


Fig. 5.9: Sketch of the helium dewar and sample rod assembly shows basic operation. Temperature of the copper plate (sample holder) is maintained by control of He gas pressure in the rod in addition to a small heater mounted on the plate.

The sample plate is shown in expanded view in Fig. 5.10. Temperature control is maintained by a feedback loop between the temperature sensor and the heater. A Lakeshore Cryotronics Temperature Controller (Model DRC81C) is used in conjunction with a Lakeshore silicon diode temperature sensor (DT-470-BO-13), and the heating element is a 63Ω , 5 W resistor which is in good thermal contact with the copper sample plate. The temperature sensor is mounted on a small copper block, which is also in good thermal contact with the sample plate. To prevent any temperature reading problems due to lead resistance, a 4-point type connection is made very close to the temperature sensor. Using this setup, the temperature is controllable to within 0.01 K for any selected temperature between 5 and 8 K.

5.6 Direction of Future Research

In this chapter the TREMBOL (transition-edge microbolometer) and the composite TREMBOL have been introduced as detectors for FIR imaging arrays. The TREMBOL utilizes a superconductor's sharp change in resistance at the normal conduction to superconduction transition. The structure of the composite bolometer enables heating of the individual detectors in an array up to their transition temperature, and can thus be used in multiplexing, which would be very advantageous for two-dimensional arrays.

Much work remains, however, to characterize the TREMBOL. A more thorough study of the Pb device is needed, perhaps with the inclusion of a polyimide passivating layer to protect the Pb from oxidizing. Other superconductors could be investigated for this application, including the high T_c superconductors. With the HT_cS , the series-added resistance structure, as well as the composite TREMBOL, could be studied.

A composite TREMBOL mask set is presently being designed which will provide for electroplated contacts on both the load/heater level and on the signal line level. It will also contain a number of test structures, including a signal line perpendicular to the bow-tie antenna. This mask set will also allow further evaluation of the composite microbolometer introduced in chapter 3.

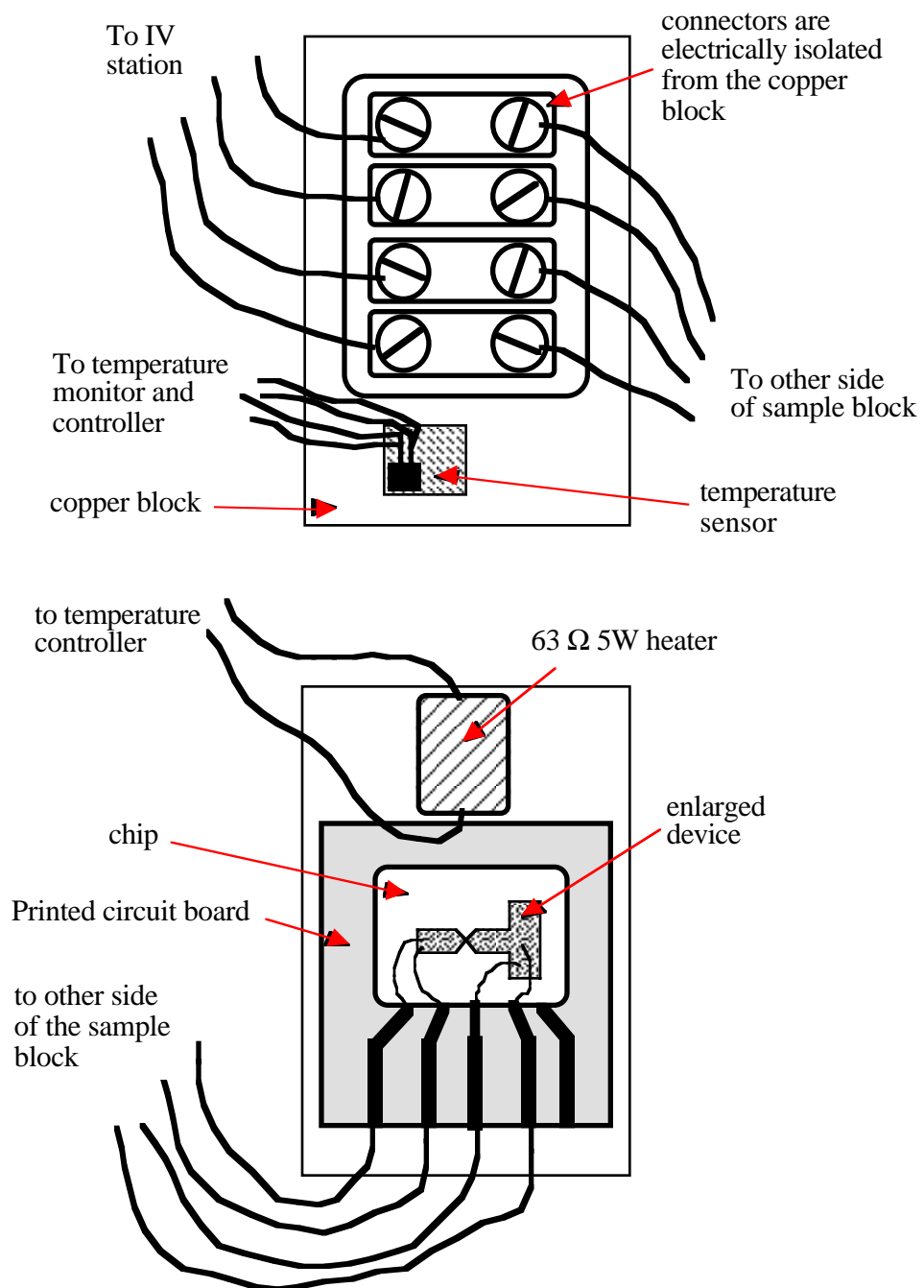


Fig. 5.10: Expanded front and back views of the 3/4" x 2" copper sample block attached to the end of the cryogenic sample rod. An enlarged representation of a wire-bonded device is also shown.

References:

- ¹. D.H. Martin and D. Bloor, "The Application of Superconductivity to the Detection of Radiant Energy," *Cryogenics*, pp. 159-165, Mar. 1961.
- ². C.L. Bertin and K. Rose, "Radiant-Energy Detection by Superconducting Films," *J. Appl. Phys.*, Vol. 39, No. 6, pp. 2561-2568, May 1968.
- ³. M.K. Maul and M.W.P. Strandberg, "Equivalent Circuit of a Superconducting Bolometer," *J. Appl. Physics*, Vol. 40, No. 7, pp. 2822-2827, June 1969.
- ⁴. G. Gallinaro and R. Varone, "Construction and calibration of a fast superconducting bolometer," *Cryogenics*, pp. 292-293, May 1975.
- ⁵. R.A. Smith, F.E. Jones, and R.P. Chasmar, The Detection and Measurement of Infrared Radiation, Oxford Univ. Press, London, 1957.
- ⁶. D.H. Andrews, R.M. Milton, and W. DeSorbo, "A Fast Superconducting Bolometer," *J. Opt. Soc. Am.*, Vol. 36, No. 9, pp. 518-524, Sep. 1946.
- ⁷. N. Fuson, "The Infra-Red Sensitivity of Superconducting Bolometers," *J. Opt. Soc. Am.*, Vol. 38, No. 10, pp. 845-853, Oct. 1948.
- ⁸. D.H. Andrews, W.F. Brucksch, Jr., W.T. Ziegler, and E.R. Blanchard, "Attenuated Superconductors: I. For Measuring Infra-Red Radiation," *Rev. Sci. Instrum.*, Vol. 13, pp. 281-292, July 1942.
- ⁹. J. Clarke, G.I. Hoffer, P.L. Richards, and N.H. Yeh, "Superconductive bolometers for submillimeter wavelengths," *J. Appl. Phys.*, Vol. 48, No. 12, pp. 4865-4879, Dec. 1977.
- ¹⁰. M. Scott, R.G. Keefe, and R. Loehman, "High Transition Temperature Superconducting Infrared Detector," *IEEE Trans. Electron Dev.*, Vol. 36, No. 1, pp. 62-65, Jan 1989.
- ¹¹. K. Rose, "Superconductive FIR Detectors," *IEEE Transactions on Electron Devices*, Vol. ED-27, No. 1, pp. 118-125, Jan. 1980.
- ¹². J.M. Lewis, "Optical Detectors Based on Superconducting Bi-Sr-Ca-Cu-Oxide Thin Films," B.S. Thesis, Mass. Inst. of Tech., June 1989.
- ¹³. K. Rose, "Superconducting Materials for Devices Spanning the Infrared-Microwave Gap," *Cryogenics*, pp. 227-230, Aug. 1969.
- ¹⁴. P.L. Richards, F. Auracher, and T. Van Duzer, "Millimeter and Submillimeter Wave Detection and Mixing with Superconducting Weak Links," *Proc. of the IEEE*, pp. 36-45, Jan. 1973.

- ¹⁵. L. Xizhi, Y. Caibing, C. Xiaoneng, F. Xizeng, S. Xiangqing, L. Shuqin, Q. Yizhi, Z. Bairo, Y. Caiwen, Z. Yinzi, Z. Yuying, L. Yong, W. Huisheg, S. Yinhuang, G. Ju, and L. Lin, "Radiant-Energy Detection By Y-Ba-Cu-O Thin Films," *Int. J. Infrared and Millimeter Waves*, pp. 445-456, 1989.
- ¹⁶. P.L. Richards, J. Clarke, R. Leoni, Ph. Lerch, S. Verghese, M.R. Beasley, T.H. Geballe, R.H. Hammond, P. Rosenthal, and S.R. Spielman, "Feasibility of the high T_C superconducting bolometer," *Appl. Phys. Lett.*, Vol. 54, No. 3, pp. 283-285, 16 Jan 1989.
- ¹⁷. D.P. Neikirk, "Integrated detector arrays for high resolution far-infrared imaging," Ph.D. thesis, California Inst. of Technol., pp. 148-149, 1984.
- ¹⁸. Q. Hu and P.L. Richards, "Design analysis of a high T_C superconducting microbolometer," *Appl. Phys. Lett.*, Vol. 55, No. 23, pp. 2444-2446, 4 Dec. 1989.
- ¹⁹. R.L. Rogers and D.P. Neikirk, "Use of Broadside Twin Element Antennas to Increase Efficiency on Electrically Thick Dielectric Substrates," *Int. J. Infrared and Millimeter Waves*, Vol. 9, No. 11, pp. 949-969, Nov 1988.
- ²⁰. S.M. Wentworth, R.L. Rogers, J.G. Heston, D.P. Neikirk, and T. Itoh, "Millimeter Wave Twin Slot Antennas on Layered Substrates," *Int. J. Infrared and Millimeter Waves*, Vol. 11, No. 2, pp. 111-131 Feb. 1990.
- ²¹. S. Baba, K. Sugawara, and A. Kinbara, "Electrical Resistivity of Thin Bismuth Films," *Thin Solid Films*, Vol. 31, pp. 329-335, 1976.
- ²². S.M. Wentworth and D.P. Neikirk, "Far-Infrared Composite Microbolometers," to be presented at the *1990 IEEE MTT-S International Microwave Symposium*, Dallas, May 8-10, 1990.
- ²³. J.G. Bednorz and K.A. Müller, "Possible High T_C Superconductivity in the Ba-La-Cu-O System," *Zeitschrift für Physik B*, Vol. 64, pp. 189-193, 1986.
- ²⁴. M.K. Wu, J.R. Ashburn, C.J. Torng, P.H. Hor, R.L. Meng, L. Gao, A.J. Huang, Y.Q. Wang, and C.W. Chu, "Superconductivity at 93 K in a New Mixed-phase Y-Ba-Cu-O Compound System at Ambient Pressure," *Phys. Rev. Lett.*, Vol. 58, No. 9, pp. 908-910, 2 Mar 1987.
- ²⁵. H. Maeda, Y. Tanaka, M. Fukutomi, and T. Asano, "A New High- T_C Oxide Superconductor without Rare Earth Element," *Jap. J. Appl. Phys.*, Vol. 27, p. L1209, 1988.

- ²⁶. M.S. Osofsky, P. Lubitz, M.Z. Harford, A.K. Singh, S.B. Qadri, E.F. Skelton, W.T. Elam, R.J. Soulen, Jr., W.L. Lechter, and S.A. Wolf, "Thin-film high T_C superconductors prepared by a simple flash evaporation technique," *Appl. Phys. Lett.*, Vol. 53, No. 17, pp. 1663-1664, 24 Oct. 1988.
- ²⁷. M. Hong, S.H. Liou, J. Kwo, and B.A. Davidson, "Superconducting Y-Ba-Cu-O oxide films by sputtering," *Appl. Phys. Lett.*, Vol. 51, No. 9, pp. 694-696, 31 Aug 1987.
- ²⁸. Z.L. Bao, F.R. Wang, Q.D. Jiang, S.Z. Wang, Z.Y. Ye, K. Wu, C.Y. Li, and D.L. Yin, "YBaCuO superconducting thin films with zero resistance at 84 K by multilayer deposition," *Appl. Phys. Lett.*, Vol. 51, No. 12, pp. 946-947, 21 Sep 1987.
- ²⁹. D.P. Neikirk, W.W. Lam, and D.B. Rutledge, "Far-Infrared Microbolometer Detectors," *Int. J. Infrared and Millimeter Waves*, Vol. 5, No. 3, pp. 245-278, Mar 1984.
- ³⁰. R.W. Simon, C.E. Platt, A.E. Lee, G.S. Lee, K.P. Daly, M.S. Wire, J.A. Luine, and M. Urbanik, "Low-loss substrate for epitaxial growth of high-temperature superconductor thin films," *Appl. Phys. Lett.*, Vol. 53, No. 26, pp. 2677-2679, 26 Dec. 1988.
- ³¹. D.B. Rutledge and M.S. Muha, "Imaging Antenna Arrays," *IEEE Trans. Ant. Prop.*, Vol. AP-30, No. 4, pp. 535-540, July 1982.
- ³². D.P. Neikirk, D.B. Rutledge, and M.S. Muha, "Far-infrared imaging antenna arrays," *Appl. Phys. Lett.*, Vol. 40, No. 3, pp. 203-205, 1 Feb. 1982.
- ³³. P.P. Tong, D.P. Neikirk, D. Psaltis, D.B. Rutledge, K. Wagner, and P.E. Young, "Tracking Antenna Arrays for Near-Millimeter Waves," *IEEE Trans. Antennas Propagat.*, Vol. AP-31, No. 3, pp. 512-515, May 1983.
- ³⁴. T.W. Bradshaw and A.H. Orlowska, "Miniature mechanical refrigerators for space use," *SPIE Vol. 915 Recent Developments in Infrared Components and Subsystems*, pp. 39-43, 1988.
- ³⁵. H. Yoshimura, M. Nagao, T. Inaguchi, T. Yamada, and M. Iwamoto, "Helium liquefaction by a Gifford-McMahon cycle cryogenic refrigerator," *Rev. Sci. Instrum.*, Vol. 60, No. 11, pp. 3533-3536, Nov. 1989.
- ³⁶. A. Owen, "Integrated Coolers: Wave of the Future," *Photonics Spectra*, pp. 148-149, Jan 1990.